International Journal of Non-Linear Mechanics ∎ (∎∎∎∎) ∎∎∎–∎∎∎

Contents lists available at ScienceDirect

International Journal of Non-Linear Mechanics

journal homepage: www.elsevier.com/locate/nlm

A structural constitutive model for smooth muscle contraction in biological tissues

Q1 Ting Tan, Raffaella De Vita

Q3 *Mechanics of Soft Biological Systems Laboratory, 330 Kelly Hall, Department of Biomedical Engineering and Mechanics, Virginia Tech, Blacksburg, VA 24061, USA*

ARTICLE INFO

Article history:
Received 12 February 2015
Accepted 20 February 2015

Keywords:
Structural constitutive model
Isometric contraction
Isotonic contraction
Biological tissues
Smooth muscle cells

ABSTRACT

A structural constitutive model that characterizes the active and passive responses of biological tissues with smooth muscle cells (SMCs) is proposed. The model is formulated under the assumption that the contractile units in SMCs and the connected collagen fibers are the active tissue active component, while the collagen fibers not connected to the SMCs are the passive tissue component. An evolution law describing the deformation of the active tissue component over time is developed based on the sliding filament theory. In this evolution law the contraction force is the sum of a motor force that initiates contraction, a viscous force that describes the actin–myosin filament sliding, and an elastic force that accounts for the deformation of the cross-bridges. The mechanical response of the collagen fibers is governed by the fiber recruitment process: collagen fibers support load and behave as a linear elastic material only after becoming taut. The proposed structural constitutive model is tested with published active and passive, uniaxial and biaxial experimental data on pig arteries.

1. Introduction

Biological hollow structures such as blood vessels, airways, gastrointestinal tracts and pelvic organs are mainly composed of an extracellular matrix and smooth muscle cells (SMCs). The extracellular matrix contains mainly elastin and collagen fibers embedded in the so-called *ground substance* and controls the passive deformation of these structures. The SMCs govern and maintain the active deformation. They have contractile units that function as sarcomeres in skeletal muscles and are composed of actin filaments, myosin filaments, and dense bodies [1,2] (Fig. 1(a)). The actin filaments are anchored to dense bodies. The dense bodies serve to connect the contractile units throughout the cell and are attached to the cell membrane [3]. Each myosin filament is aligned between two actin filaments, with the myosin heads uniformly spaced between these filaments [3]. When the intracellular calcium concentration increases due to electric, chemical, and mechanical stimuli, cross-bridges form between the myosin heads and the actin filaments, leading to SMC contraction [4]. SMCs generate a contraction force that is comparable to the force generated by skeletal muscle cells. However, unlike skeletal muscle cells, SMCs maintain this contraction force over a longer time, and they have a much lower contraction speed so as to accomplish their physiological functions (e.g., maintain proper pressure in blood vessels, propelling food in the gastrointestinal tracts) [5].

The contraction mechanism in skeletal muscle has been explained by H.E. Huxley, A.F. Huxley and co-authors [6–9], who proposed the so-called *sliding-filament theory*. According to this theory, the contraction force in skeletal muscle is generated by the attachment of myosin heads to actin filaments (i.e., the formation of cross-bridges) during actin–myosin filament sliding. Based on the sliding-filament theory, Hai and Murphy presented a new model that includes the *latch state* introduced by Dillon et al. [10,11] to capture the characteristic cross-bridge kinetics of the SMCs [12]. In this state, a high contraction force is maintained at a very low or even zero contraction speed.

Constitutive models that describe the active mechanical contribution of SMCs in biological hollow structures have been proposed over the years. The passive response has been usually assumed to be due to the collagen and elastin fibers, while the active response has been assumed to be determined by the contractile units in SMCs. For vascular tissue, Rachev and Hayashi [13] introduced an *ad hoc* parameter that defined the contractile activity of SMCs to model the active stress, and adopted a parabolic function for the typical isometric length–tension data. Later, Zulliger et al. [14] proposed a structural model for arteries that included the mechanical contribution of SMCs. The active stress was defined by introducing two functions that described the muscle tone level and the isometric length–tension data. To more precisely account for the contraction mechanisms of SMCs, a mechano-chemical model considering Ca^{2+} concentration and temperature was proposed by Stålhand et al. [15]. In this model, the SMC deformation was assumed to be the result of cross-bridge deformation and filament sliding. Recently, Murtada et al. [16,17]

E-mail address: devita@vt.edu (R. De Vita).

http://dx.doi.org/10.1016/j.ijnonlinmec.2015.02.009
0020-7462/

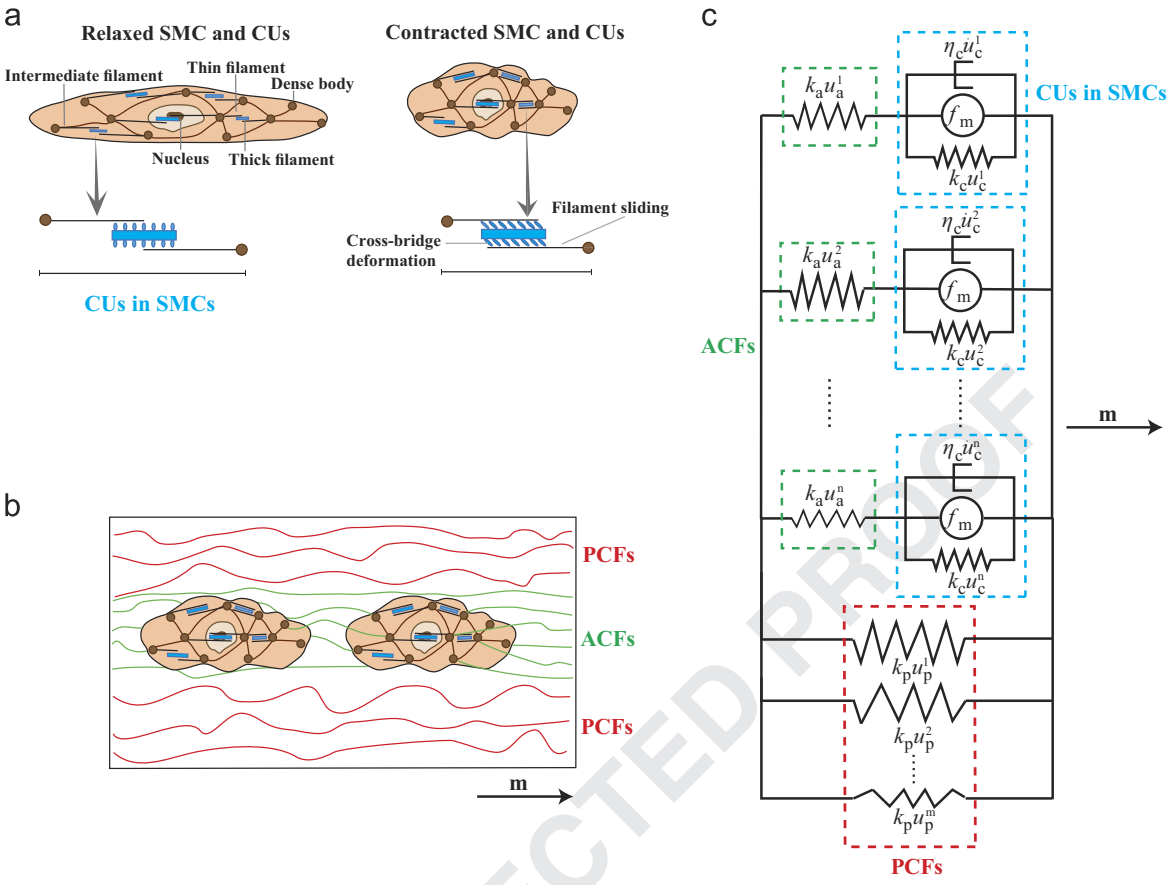

Fig. 1. (a) Smooth muscle cells (SMCs) and contractile units (CUs). (b) Active collagen fibers (ACFs), passive collagen fibers (PCFs), and SMCs. (c) Model schematic for PCFs, ACFs, and CUs in SMCs showing only a discrete number of elements: n elements for the ACFs (or CUs) and m elements for the PCFs. In the proposed model, the continuous recruitment of these elements under load is described by a probability density function. *Note:* All the elements are oriented along the unit vector **m** in the reference configuration.

proposed a new theoretical framework in which the active response was defined by considering the dispersion of contractile units, actin–myosin filament overlap and sliding, and chemical activity as done by Hai and Murphy [12]. More specifically, they introduced a phenomenological parabolic filament overlap function [17], which captured the length–tension data in isometric experiments. Finally, Chen et al. [18] developed a constitutive model that also incorporated the experimentally measured orientation of vascular SMCs.

In this study, a new structural constitutive model for the active and passive mechanical behavior of biological tissues containing SMCs is proposed. The SMC contraction force is assumed to be equal to the force acting on the surrounding collagen fibers. This assumption is justified by the fact that the contraction force generated by SMCs can be transmitted, via their connection to the dense bodies, to the extracellular matrix [1]. Thus, the active stress can be computed from the stress of the collagen fibers that are connected to the SMCs, without introducing a chemical kinetics model as done by other investigators [16,17]. Within the framework of Hill's three-element model [19], we develop an evolution law for the deformation of SMCs and connected collagen fibers. Following the sliding filament theory, in this evolution law the contraction force is the sum of a motor force that initiates contraction, a viscous force that describes the actin–myosin filament sliding, and an elastic force that accounts for the cross-bridge deformation. The passive response of the collagen fibers is captured by the non-linear elastic model proposed by De Vita et al. [20]. The proposed structural constitutive model is then tested using uniaxial isometric length–tension [17] and isotonic quick-release experimental data [10] on pig carotid arteries and biaxial isometric inflation–extension experimental data on pig coronary arteries [18].

2. Model formulation

In the proposed model, the mechanical behavior of biological tissues with SMCs is assumed to be determined by the collagen fibers. We assume that there are two different types of collagen fibers based on their interaction with SMCs (Fig. 1(b)). Collagen fibers of the first type are directly connected to SMCs. These collagen fibers determine the active mechanical response of the tissues. The activation of SMCs is assumed to be transmitted to the neighboring collagen fibers. For this reason, the collagen fibers connected to SMCs are called the *active collagen fibers* (ACFs). Collagen fibers of the second type are not connected to SMCs. These determine the passive mechanical response of the tissues and are called the *passive collagen fibers* (PCFs). The mechanical contributions of other components (e.g., ground substance or elastin) are neglected. In summary, the active and passive mechanical behaviors of biological tissues with SMCs are determined by the ACFs and PCFs, respectively.

2.1. Constitutive model for the ACFs and PCFs

Within the framework of non-linear elasticity, the active or passive first and second Piola–Kirchhoff stress tensors, **P** and **S**, respectively, are expressed as [21]

$$\mathbf{P} = -p\mathbf{F}^{-\mathrm{T}} + 2\mathbf{F}\cdot\frac{\partial W}{\partial \mathbf{C}}, \quad \mathbf{S} = -p\mathbf{C}^{-1} + 2\frac{\partial W}{\partial \mathbf{C}}, \tag{1}$$

where p is the Lagrange multiplier that accounts for incompressibility, **F** is the deformation gradient, $\mathbf{C} = \mathbf{F}^{\mathrm{T}}\cdot\mathbf{F}$ is the right Cauchy–Green strain tensor, and W is the strain energy of ACFs

Please cite this article as: T. Tan, R. De Vita, A structural constitutive model for smooth muscle contraction in biological tissues, International Journal of Non-Linear Mechanics (2015), http://dx.doi.org/10.1016/j.ijnonlinmec.2015.02.009

or PCFs, which can be defined as

$$W = \int_{\Sigma} R(\mathbf{m}) w(\lambda(\mathbf{C}, \mathbf{m}))\, \mathrm{d}\Sigma, \tag{2}$$

where Σ is the set of all material directions, $R(\mathbf{m})$ is the probability density function for ACFs or PCFs with mean axis being parallel to the unit vector $\mathbf{m}$ in the reference configuration, w is the strain energy of ACFs or PCFs along $\mathbf{m}$, and $\lambda(\mathbf{C}, \mathbf{m}) = \sqrt{\mathbf{m} \cdot \mathbf{C} \cdot \mathbf{m}}$ is the ACF or PCF axial stretch. After defining the ACF or PCF axial stress as $\sigma = \mathrm{d}w/\mathrm{d}\lambda$, the first and second Piola–Kirchhoff stress tensors in Eq. (1) can be rewritten as

$$\mathbf{P} = -p\mathbf{F}^{-\mathrm{T}} + \mathbf{F} \cdot \int_{\Sigma} R(\mathbf{m}) \frac{\sigma}{\lambda} \mathbf{m} \otimes \mathbf{m}\, \mathrm{d}\Sigma,$$
$$\mathbf{S} = -p\mathbf{C}^{-1} + \int_{\Sigma} R(\mathbf{m}) \frac{\sigma}{\lambda} \mathbf{m} \otimes \mathbf{m}\, \mathrm{d}\Sigma. \tag{3}$$

Both ACFs and PCFs are assumed to support load only after becoming taut and are linear elastic with elastic modulus K, as done in our previous work [20]. A Weibull probability density function with shape parameter κ, scale parameter γ, and location parameter of 1 is then introduced to model the gradual straightening and recruitment of collagen fibers. Then, the axial stress σ of ACFs or PCFs is expressed as [20]

$$\sigma = \int_{\lambda_1}^{\lambda_2} \frac{\kappa}{\gamma^{\kappa}} (\lambda_{\mathrm{t}} - 1)^{\kappa - 1} \mathrm{e}^{-((\lambda_{\mathrm{t}} - 1)/\gamma)^{\kappa}} K\left(\frac{\lambda}{\lambda_{\mathrm{t}}} - 1\right) \mathrm{d}\lambda_{\mathrm{t}}, \tag{4}$$

where λ_{t} is the stretch at which the ACFs or PCFs become taut, and λ_1 and λ_2 are the lower and upper bounds for λ_{t}, respectively. It must be noted that the above equations describe both the active and passive mechanical responses of the tissue. In the sections below, two subscripts, "a" and "p," will be introduced to distinguish active and passive axial stretches, which lead to active and passive stresses for axisymmetric deformations. Thus, λ_{a} will denote the axial stretch for ACFs and λ_{p} will denote the axial stretch for PCFs.

2.2. Evolution law

The axial stretch of ACFs, λ_{a}, along the direction $\mathbf{m}$ is a function of the SMC contraction time t. In order to determine this function, which is also known as the evolution law, we assume that, along $\mathbf{m}$, SMCs and ACFs are subjected to the same force due to their connections and, therefore, are arranged in series (Fig. 1(c)). Within the contractile units in SMCs, the actin–myosin filament sliding is assumed to generate a viscous force and the cross-bridge deformation is assumed to generate an elastic force. The viscous force is modeled using a dashpot element and the elastic force using a spring element. Moreover, the existence of a motor force that initiates SMC contraction is postulated as done by other investigators [16]. SMCs that are connected to ACFs along the direction $\mathbf{m}$ are thus modeled as a combination of three parallel elements (Fig. 1(c)). As mentioned in Section 2.1, ACFs are assumed to be linear elastic and are modeled as a spring element. Because along $\mathbf{m}$ the ACFs are arranged in series with the contractile units of SMCs, one has

$$k_{\mathrm{a}} u_{\mathrm{a}}(t) = \eta_{\mathrm{c}} \dot{u}_{\mathrm{c}}(t) + k_{\mathrm{c}} u_{\mathrm{c}}(t) + f_{\mathrm{c}}, \tag{5}$$

where k_{a} and $u_{\mathrm{a}}(t)$ are the spring stiffness and axial displacement of the ACFs, respectively, η_{c}, k_{c}, $u_{\mathrm{c}}(t)$, and f_{c} are the viscous coefficient, spring stiffness, axial displacement, and motor force of the contractile units, respectively, and t is the contraction time. We emphasize that u_{a} in Eq. (5) is the axial displacement of the ACFs (and not the axial displacement of the *taut* ACFs). We also note that the ACFs contribute to the total active stress only when they are taut and, in that case, they behave as a linear elastic material. However, during SMC contraction, the ACFs generate a force, which is equal to the force in the SMCs, even when they are not taut. This force will not contribute to the total active stress of the tissue unless the ACFs are taut.

Along the direction $\mathbf{m}$, PCFs are modeled as springs that are parallel to the series of ACFs and contractile units (Fig. 1(c)). Thus, $u_{\mathrm{a}}(t)$ and $u_{\mathrm{c}}(t)$ are related to the axial stretch of PCFs, $\lambda_{\mathrm{p}}(t)$, by

$$\lambda_{\mathrm{p}}(t) = \frac{L_0 + u_{\mathrm{a}}(t) + u_{\mathrm{c}}(t)}{L_0}, \tag{6}$$

where L_0 is the original length of PCFs. We assume that the axial stretch of the PCFs is equal to the axial stretch of the tissue along $\mathbf{m}$ and can be expressed as

$$\lambda_{\mathrm{p}}(t) = \begin{cases} \lambda_{\mathrm{m}} & \text{for isometric contraction,} \\ \lambda_{\mathrm{m}} + \frac{V(\mathrm{e}^{-\mu t} - 1)}{\mu} & \text{for isotonic contraction,} \end{cases} \tag{7}$$

where λ_{m} is the constant tissue stretch along $\mathbf{m}$ in isometric experiments, V is the normalized initial velocity of the tissue with respect to L_0 in isotonic experiments, and μ is a constant parameter that controls the rate and amount of change of the constant stretch. Note that, for the isotonic experiments, $\lambda_{\mathrm{p}}(t)$ can be obtained by integrating the axial velocity of the PCFs, i.e. $\dot{\lambda}_{\mathrm{p}}(t) = -V\mathrm{e}^{-\mu t}$. This exponential decaying function for the axial stretch of PCFs is assumed based on experimental data and previous models [22,23].

2.3. Isometric contraction

For isometric contraction, $\lambda_{\mathrm{p}}(t) = \lambda_{\mathrm{m}}$. After replacing $\lambda_{\mathrm{p}}(t)$ with λ_{m} in Eq. (6), one can express u_{a} in terms of u_{c}, λ_{m}, and L_0 then substitute it into Eq. (5). The solution of the resulting differential equation, $u_{\mathrm{c}}(t)$, has the following form:

$$u_{\mathrm{c}}(t) = \beta(f - \lambda_{\mathrm{m}} + 1)(\mathrm{e}^{-\alpha t} - 1)L_0 + u_{\mathrm{c}}(0)\mathrm{e}^{-\alpha t}, \tag{8}$$

where $\alpha = (k_{\mathrm{a}} + k_{\mathrm{c}})/\eta_{\mathrm{c}}$, $\beta = k_{\mathrm{a}}/(k_{\mathrm{c}} + k_{\mathrm{a}})$, and $f = f_{\mathrm{c}}/k_{\mathrm{s}}L_0$. The initial axial displacement of the SMC contractile units is unknown from the experiments, so we assume that

$$u_{\mathrm{c}}(0) = a(\lambda_{\mathrm{m}} - 1)L_0, \tag{9}$$

where $0 \le a \le 1$ is a fractional length parameter. This assumption implies that the initial axial displacement of the SMC contractile units is a fraction of the axial tissue displacement. After introducing the parameter a, the axial stretch of ACFs can then be written as

$$\lambda_{\mathrm{a}}(t) = 1 + \frac{u_{\mathrm{a}}(t)}{(1 - a)L_0}. \tag{10}$$

By substituting Eq. (8) into Eq. (6), one obtains $u_{\mathrm{a}}(t)$. This can then be substituted into Eq. (10) so that, for an isometric contraction,

$$\lambda_{\mathrm{a}}(t) = 1 + \frac{(\lambda_{\mathrm{m}} - 1)(1 - a\mathrm{e}^{-\alpha t}) + \beta[f - (\lambda_{\mathrm{m}} - 1)](1 - \mathrm{e}^{-\alpha t})}{1 - a}. \tag{11}$$

2.4. Isotonic contraction

For isotonic contraction, $\lambda_{\mathrm{p}}(t) = \lambda_{\mathrm{m}} + V(\mathrm{e}^{-\mu t} - 1)/\mu$, where λ_{m} is the constant tissue stretch in isometric experiments. This expression for $\lambda_{\mathrm{p}}(t)$ can be substituted in Eq. (6) and u_{a} can be written in terms of u_{c}, λ_{m}, and L_0 and then substitute it into Eq. (5). The solution of the resulting differential equation, $u_{\mathrm{c}}(t)$, has the following form:

$$u_{\mathrm{c}}(t) = \beta(f - \lambda_{\mathrm{m}} + 1)(\mathrm{e}^{-\alpha\tilde{t}} - 1)L_0 + a(\lambda_{\mathrm{m}} - 1)L_0\mathrm{e}^{-\alpha\tilde{t}} + VL_0\beta\left[\frac{\mathrm{e}^{-\mu t} - 1}{\mu} - \frac{\mathrm{e}^{-\mu t} - \mathrm{e}^{-\alpha t}}{\mu - \alpha}\right], \tag{12}$$

where α, β, f, L_0, a are defined as above, and $\tilde{t}$ is a constant that represents the duration of the isometric contraction that precedes the isotonic contraction. The first two terms of the right-hand side

Please cite this article as: T. Tan, R. De Vita, A structural constitutive model for smooth muscle contraction in biological tissues, International Journal of Non-Linear Mechanics (2015), http://dx.doi.org/10.1016/j.ijnonlinmec.2015.02.009

of Eq. (12) represent the axial displacement of the contractile units at the end of the isometric contraction (i.e., Eq. (8) evaluated at $t=\tilde{t}$).

By substituting Eq. (12) into Eq. (6), one obtains $u_a(t)$ for an isotonic contraction. This can then be substituted into Eq. (10), so that $\lambda_a(t)$ for an isotonic contraction becomes

$$\lambda_a(t)=1+\frac{(\lambda_m-1)(1-ae^{-\alpha\tilde{t}})+\beta[f-(\lambda_m-1)](1-e^{-\alpha\tilde{t}})}{1-a}+\frac{V}{1-a}\left[\frac{(1-\beta)(e^{-\mu t}-1)}{\mu}+\frac{\beta(e^{-\mu t}-e^{-\alpha t})}{\mu-\alpha}\right]. \quad (13)$$

Again, we note that the first two terms of the right-hand side of Eq. (13) represent the axial stretch of the ACFs at the end of the isometric contraction (i.e., Eq. (11) evaluated at $t=\tilde{t}$).

3. Model implementation

3.1. Reduced 1-D model

In order to test the constitutive model with published uniaxial data collected from isometric and isotonic experiments on carotid arteries [17,10], we assume that the tested specimens undergo a homogeneous isochoric axisymmetric deformation. Thus, the deformation gradient of the ACFs or PCFs has the following form:

$$\mathbf{F}=\lambda^{-1/2}\mathbf{e}_1\otimes\mathbf{E}_1+\lambda^{-1/2}\mathbf{e}_2\otimes\mathbf{E}_2+\lambda\mathbf{e}_3\otimes\mathbf{E}_3, \quad (14)$$

where λ is the axial stretch of the ACFs or PCFs. The orthonormal bases $\{\mathbf{E}_1,\mathbf{E}_2,\mathbf{E}_3\}$ and $\{\mathbf{e}_1,\mathbf{e}_2,\mathbf{e}_3\}$ are defined so that the $\mathbf{E}_3$ and $\mathbf{e}_3$ are the loading directions in the reference and current configurations, respectively.

In the reference configuration, the ACFs or PCFs are assumed to be all aligned along the loading direction $\mathbf{E}_3$. Thus, in Eq. (3), $R(\mathbf{m})=\delta(\mathbf{m}-\mathbf{E}_3)$, where δ is the Dirac delta function. Substituting Eqs. (4) and (15) into Eq. (3), the non-zero components of the active or passive first Piola–Kirchhoff stress tensor are the following:

$$P_{11}=P_{22}=-p\lambda^{-1/2},\quad P_{33}=-p\lambda^{-1/2}+\sigma(\lambda). \quad (15)$$

After applying the traction-free boundary condition $P_{11}=P_{22}=0$ on the lateral surface of the specimens, we obtain $p=0$. Thus, the constitutive equation that defines the response of the ACFs or PCFs is

$$P_{33}(\lambda)=\sigma(\lambda)=\int_{\lambda_1}^{\lambda_2}\frac{\kappa}{\gamma^\kappa}(\lambda_t-1)^{\kappa-1}e^{-((\lambda_t-1)/\gamma)^\kappa}K\left(\frac{\lambda}{\lambda_t}-1\right)d\lambda_t. \quad (16)$$

The above equation defines the response of the ACFs for $\lambda=\lambda_a(t)$, $\lambda_1=\lambda_m$, and $\lambda_2=\lambda_a(t)$. More specifically, for an isometric contraction $\lambda_a(t)$ is given by Eq. (11) and for an isotonic contraction $\lambda_a(t)$ is given by Eq. (13). Eq. (16) also defines the response of the PCFs for $\lambda=\lambda_p(t)$, $\lambda_1=1$, and $\lambda_2=\lambda_p(t)$ where $\lambda_p(t)$ is given by Eq. (7). The total stress of the tissue is obtained as the sum of the stress of ACFs, $P_{33}(\lambda_a)$, and the stress of PCFs, $P_{33}(\lambda_p)$. We note that the model parameters κ, γ, and K in Eq. (16) are assumed to have the same values for both ACFs and PCFs.

3.2. Reduced 2-D model

The constitutive model proposed is also tested with biaxial data that are obtained from isometric inflation–extension tests on coronary arteries. Thus, we assume that the specimens undergo a homogeneous isochoric axisymmetric deformation defined by

$$\mathbf{F}=(\lambda_\theta\lambda_z)^{-1}\mathbf{e}_r\otimes\mathbf{E}_R+\lambda_\theta\mathbf{e}_\theta\otimes\mathbf{E}_\Theta+\lambda_z\mathbf{e}_z\otimes\mathbf{E}_z, \quad (17)$$

where λ_θ and λ_z are the circumferential stretch and axial stretch of the ACFs or PCFs, respectively. The orthonormal bases $\{\mathbf{E}_R,\mathbf{E}_\Theta,\mathbf{E}_z\}$ and $\{\mathbf{e}_R,\mathbf{e}_\Theta,\mathbf{e}_z\}$ are defined so that the $\mathbf{E}_R$, $\mathbf{E}_z$ and $\mathbf{e}_R$, $\mathbf{e}_z$ are the biaxial loading directions in the reference and current configurations, respectively. In the reference configuration, the collagen fibers are assumed to be aligned in two preferred directions $\mathbf{m}_1=\cos(\psi)\mathbf{E}_\theta+\sin(\psi)\mathbf{E}_z$ and $\mathbf{m}_2=\cos(\psi)\mathbf{E}_\theta-\sin(\psi)\mathbf{E}_z$, where ψ and $-\psi$ are the angles off the circumferential axis $\mathbf{E}_\Theta$. Then, $R(\mathbf{m})=(\delta(\mathbf{m}-\mathbf{m}_1)+\delta(\mathbf{m}-\mathbf{m}_2))/2$ and the strain energy in Eq. (2) can be re-written as

$$W=\frac{w(\lambda(\mathbf{C},\mathbf{m}_2))+w(\lambda(\mathbf{C},\mathbf{m}_1))}{2}, \quad (18)$$

where $\lambda(\mathbf{C},\mathbf{m}_1)$ and $\lambda(\mathbf{C},\mathbf{m}_2)$ are the axial stretches of the fibers. It then follows from Eqs. (7), (11), and (13) that since $\lambda_m(\mathbf{C},\mathbf{m}_1)=\lambda_m(\mathbf{C},\mathbf{m}_2)=\sqrt{\lambda_\theta^2\cos^2\psi+\lambda_z^2\sin^2\psi}$, then $\lambda(\mathbf{C},\mathbf{m}_1)=\lambda(\mathbf{C},\mathbf{m}_2)$. Then the axial stresses along $\mathbf{m}_1$ and $\mathbf{m}_2$ defined by Eq. (4) are equal: $\sigma(\lambda(\mathbf{C},\mathbf{m}_1))=\sigma(\lambda(\mathbf{C},\mathbf{m}_2))$.

Substituting Eqs. (4) and (18) into Eq. (3), one gets the following non-zero components of the second Piola–Kirchhoff stress tensor:

$$S_{rr}=-p(\lambda_\theta\lambda_z)^2,\quad S_{\theta\theta}=\frac{\sigma(\lambda)}{\lambda}\cos^2(\psi)-\frac{p}{\lambda_\theta^2},\quad S_{zz}=\frac{\sigma(\lambda)}{\lambda}\sin^2(\psi)-\frac{p}{\lambda_z^2}. \quad (19)$$

By following Fung et al. [24], we assume that $S_{rr}=0$ and, hence, $p=0$. Then, it follows that

$$S_{\theta\theta}=\frac{\sigma(\lambda)}{\lambda}\cos^2(\psi),\quad S_{zz}=\frac{\sigma(\lambda)}{\lambda}\sin^2(\psi), \quad (20)$$

where

$$\sigma(\lambda)=\int_{\lambda_1}^{\lambda_2}\frac{\kappa}{\gamma^\kappa}(\lambda_t-1)^{\kappa-1}e^{-((\lambda_t-1)/\gamma)^\kappa}K\left(\frac{\lambda}{\lambda_t}-1\right)d\lambda_t. \quad (21)$$

(Eqs. (20) and (21)) define the non-zero components of the second Piola–Kirchhoff stress tensor of the ACFs for $\lambda=\lambda_a(t)$, $\lambda_1=\lambda_m$, and $\lambda_2=\lambda_a(t)$, where $\lambda_a(t)$ is given by Eq. (11). Eqs. (20) and (21) are the non-zero components of the second Piola–Kirchhoff stress tensor of the PCFs for $\lambda=\lambda_p(t)$, $\lambda_1=1$, and $\lambda_2=\lambda_p(t)$, where $\lambda_p(t)$ is given by Eq. (7)$_1$. Again, the model parameters, κ, γ, and K, in Eq. (21) are assumed to have the same values for both ACFs and PCFs.

3.3. Parameter determination

The model parameters were identified by using three sets of published experimental data on pig arteries that were obtained by performing uniaxial isometric length–tension tests [17], uniaxial isometric and isotonic quick-release tests [10], and biaxial isometric inflation–extension tests [18]. These parameters were calculated by minimizing three different error functions, as described in detail below, using the *fmincon* function with the *interior-point method* in MATLAB (MATLAB R2013b, MathWorks). All the model parameters were constrained to be non-negative. Furthermore, the parameters a satisfied the inequality $0\le a\le 1$.

When using the isometric length–tension data [17], the seven parameters $\{\alpha, \beta, a, f, \kappa, \gamma, K\}$ were obtained by minimizing the error function, Er_1, defined as

$$Er_1=\sum_{\lambda_m}(P_{33}^{exp}(\lambda_a(\lambda_m))-P_{33}^{theor}(\lambda_a(\lambda_m)))^2+\sum_{\lambda_m}(P_{33}^{exp}(\lambda_p(\lambda_m))-P_{33}^{theor}(\lambda_p(\lambda_m)))^2+\sum_{t}(P_{33}^{exp}(\lambda_a(t))-P_{33}^{theor}(\lambda_a(t)))^2, \quad (22)$$

where $P_{33}^{exp}(\lambda_a(\lambda_m))$ and $P_{33}^{theor}(\lambda_a(\lambda_m))$ are the experimental and theoretical non-zero components of the first Piola–Kirchhoff stress tensor for the ACFs, respectively, and $P_{33}^{exp}(\lambda_p(\lambda_m))$ and $P_{33}^{theor}(\lambda_p(\lambda_m))$

Please cite this article as: T. Tan, R. De Vita, A structural constitutive model for smooth muscle contraction in biological tissues, International Journal of Non-Linear Mechanics (2015), http://dx.doi.org/10.1016/j.ijnonlinmec.2015.02.009

are the experimental and theoretical non-zero components of the first Piola–Kirchhoff stress tensor for the PCFs, respectively. We note that the active and passive stretches, λ_a and λ_p, are functions of the tissue stretch λ_m via Eqs. (11) and $(7)_1$, respectively. Experimentally, the stresses were always measured at a contraction time $t=300$ s. $P_{33}^{exp}(\lambda_a(t))$ and $P_{33}^{theor}(\lambda_a(t))$ are the experimental and theoretical non-zero components of the first Piola–Kirchhoff stress tensor for the ACFs, respectively. These vary with the contraction time t for a constant tissue stretch $\lambda_m = 1.5$.

Uniaxial isometric and isotonic experimental data [11] were also used to compute the model parameters. Toward this end, the eight model parameters $\{\alpha, \beta, a, f, \kappa, \gamma, K, \mu\}$ were identified by minimizing the error function, Er_2, defined as

$$Er_2 = \sum_t (P_{33}^{exp}(\lambda_a(t)) - P_{33}^{theor}(\lambda_a(t)))^2 + \sum_V ((F/F_0)^{exp}(V) - (F/F_0)^{theor}(V))^2, \quad (23)$$

where $P_{33}^{exp}(\lambda_a(t))$ and $P_{33}^{theor}(\lambda_a(t))$ are the isometric experimental and theoretical non-zero components of the first Piola–Kirchhoff stress tensor for the ACFs at a constant $\lambda_m = 1.6$, respectively. These components change with the contraction time t. $(F/F_0)^{exp}(V)$ and $(F/F_0)^{theor}(V)$ define the experimental and theoretical normalized forces applied to the tissue during isotonic experiments as functions of the isotonic initial velocities V computed at a constant $\lambda_m = 1.6$ and constant contraction time $t=3000$ s. F/F_0 is the normalized force with respect to the maximum force F_0 obtained in isometric experiments. It is equal to the ratio of the total stress, $P_{33}(\lambda_a(V)+P_{33}(\lambda_p(V)))$, in isotonic experiments and the total stress obtained in isometric experiments, which was reported to be 290 kPa. We note that λ_a and λ_p depend on V via Eqs. (13) and $(7)_2$, respectively.

Biaxial isometric data from inflation–extension tests [18] were used to evaluate the eight model parameters $\{\alpha, \beta, a, f, \kappa, \gamma, K, \psi\}$. The following error function, Er_3, was minimized:

$$\begin{aligned} Er_3 = \sum_{\lambda_\theta} \{ & [(S_{\theta\theta}^{exp}(\lambda_a(\lambda_\theta)) - S_{\theta\theta}^{theor}(\lambda_a(\lambda_\theta)))^2 + (S_{zz}^{exp}(\lambda_a(\lambda_\theta)) \\ & - S_{zz}^{theor}(\lambda_a(\lambda_\theta)))^2 \\ & + (S_{\theta\theta}^{exp}(\lambda_p(\lambda_\theta)) - S_{\theta\theta}^{theor}(\lambda_p(\lambda_\theta)))^2 + (S_{zz}^{exp}(\lambda_p(\lambda_\theta)) \\ & - S_{zz}^{theor}(\lambda_p(\lambda_\theta)))^2]|_{\lambda_z = 1.2} \\ & + [(S_{\theta\theta}^{exp}(\lambda_a(\lambda_\theta)) - S_{\theta\theta}^{theor}(\lambda_a(\lambda_\theta)))^2 + (S_{zz}^{exp}(\lambda_a(\lambda_\theta)) - S_{zz}^{theor}(\lambda_a(\lambda_\theta)))^2 \\ & + (S_{\theta\theta}^{exp}(\lambda_p(\lambda_\theta)) - S_{\theta\theta}^{theor}(\lambda_p(\lambda_\theta)))^2 + (S_{zz}^{exp}(\lambda_p(\lambda_\theta)) \\ & - S_{zz}^{theor}(\lambda_p(\lambda_\theta)))^2]|_{\lambda_z = 1.3} \}, \end{aligned} \quad (24)$$

where $S_{\theta\theta}^{exp}(\lambda_a(\lambda_\theta))$ and $S_{\theta\theta}^{theor}(\lambda_a(\lambda_\theta))$ are the experimental and theoretical circumferential components of the second Piola–Kirchhoff stress tensor for the ACFs, respectively, and $S_{zz}^{exp}(\lambda_a(\lambda_\theta))$ and $S_{zz}^{theor}(\lambda_a(\lambda_\theta))$ are the experimental and theoretical axial components of the second Piola–Kirchhoff stress tensor for the ACFs, respectively. $S_{\theta\theta}^{exp}(\lambda_p(\lambda_\theta))$ and $S_{\theta\theta}^{theor}(\lambda_p(\lambda_\theta))$ are the experimental and theoretical circumferential components of the second Piola–Kirchhoff stress tensor for the PCFs, respectively, and $S_{zz}^{exp}(\lambda_p(\lambda_\theta))$ and $S_{zz}^{theor}(\lambda_p(\lambda_\theta))$ are the experimental and theoretical axial components of the second Piola–Kirchhoff stress tensor for the PCFs, respectively. The active and passive stretches, λ_a and λ_p, are functions of the circumferential tissue stretch λ_θ at a constant axial tissue stretch λ_z of 1.2 or 1.3. The stresses were always measured experimentally at a constant contraction time $t=900$ s.

4. Results

In the study by Murtada et al. [17], active and passive stress–stretch data were collected from strips of pig carotid media arteries in the circumferential direction. Stretch data were computed by normalizing the tissue length with respect to the tissue length in the slack configuration. It must be noted that, although isometric length–tension data have been published by several investigators [4,25,26], the stretch of the tissue is often measured as the tissue length normalized with respect to the optimal length, i.e. the length at the maximal active tension. The data reported by Murtada et al. [17] captured the tissue deformation independent of the tested specimen's dimensions and optimal length. For this reason, these data were selected to compute the model parameters in Eqs. (11) and (16).

The digitized experimental data and our model fit are shown in Fig. 2. The values of the model parameters are reported in Table 1. Active stress–time data recorded at an optimal stretch of 1.5 were presented by Murtada et al. [17]. The constitutive model fits well these data: it captures the increase in the active stress with the contraction time of SMCs (Fig. 2(a)). The active stress was found to be almost constant after reaching its maximum value at 200 s. In Fig. 2 (b), the digitized active and passive stress–stretch data and model fits are shown. The constitutive model describes well the typical passive non-linear elastic response of soft biological tissues. It also reproduces the increase in active stress with tissue stretch and the decrease in active stress after reaching the maximum value at the optimal stretch. The coefficient of determination R^2 was found to be 0.862. Considering the variation in the active and passive stress–stretch experimental data, the constitutive model appears to be capable of fitting the uniaxial isometric experimental data by Murtada et al. [17].

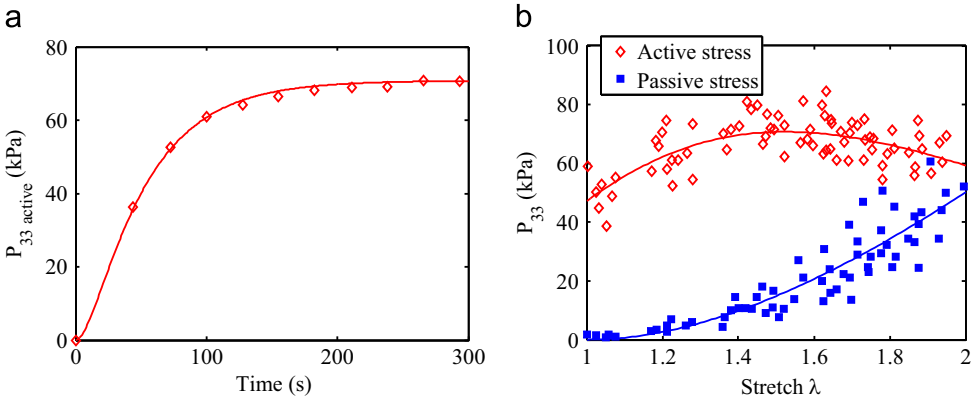

Fig. 2. Active and passive uniaxial data [17] and model fits ($R^2=0.862$). (a) Active stress–time experimental data (red symbols) at a stretch of 1.5 and model fit (continuous line); (b) Active and passive stress–stretch data (blue and red symbols, respectively) and model fit (continuous lines). (For interpretation of the references to color in this figure caption, the reader is referred to the web version of this paper.)

Please cite this article as: T. Tan, R. De Vita, A structural constitutive model for smooth muscle contraction in biological tissues, International Journal of Non-Linear Mechanics (2015), http://dx.doi.org/10.1016/j.ijnonlinmec.2015.02.009

Uniaxial isometric data obtained from length–tension experiments and uniaxial isotonic data obtained from quick-release experiments on swine carotid media specimens were reported by Dillon et al. [10]. We note that many experimental studies have focused on determining either isometric length–tension relationships or isotonic force–velocity relationships [4,11,22,12]. However, since both isometric and isotonic data were reported by Dillon et al. [10], these data were selected and used simultaneously to determine the model parameters in Eqs. (7), (13), and (16). The digitized active stress–time experimental data at an optimal stretch of 1.6 [10] and the model fit are shown in Fig. 3(a). The constitutive law with the values of the model parameters reported in Table 1 reproduces the results of the experiments: there is a quick increase in the active stress followed by a plateau region that starts at around 100 s. The model also successfully illustrates the non-linear force–velocity relationship, which is characterized by a decrease in velocity with increasing force while the tissue isshortening (Fig. 3(b)). Overall, the proposed model can simulate the uniaxial isometric and isotonic behavior of pig carotid arteries ($R^2=0.922$).

Recently, biaxial mechanical data for pig coronary arteries obtained from inflation–extension experiments were presented by Chen et al. [18]. To our knowledge, among published data, this is the most complete set of experimental data that characterizes the biaxial active and passive stress–stretch relationships [27–29]. For this reason, we utilized these experimental data to determine the model parameters in Eqs. (20) and (21). In Fig. 4, both the digitized active and passive experimental stress data collected in circumferential and axial directions under a constant axial stretch of 1.2 or 1.3 are plotted versus the circumferential stretch with the model fits. The biaxial passive and active stress–stretch relationships are well captured by the model. The values of the model parameters are reported in Table 1. The R^2 was found to be 0.965. As expected, the axial stresses are found to be lower than the circumferential ones. This can be explained by the collagen fiber preferred orientation of 37° off the circumferential direction (see Table 1). That is to say, the tissue is anisotropic. It is stiffer in the circumferential direction than in the axial direction.

5. Discussion

In recent years, mechano-chemical constitutive models that account for the chemical states of myosin have been developed for SMC contraction based on the so-called *four-state chemical model* [15,30,17]. In these models, the active stress of biological tissues depends on the number of activated myosin heads and their stiffness. This number is obtained from chemical kinetics models. In the constitutive model proposed by Kroon [30], five chemical parameters were fixed based on the work by Hai and Murphy [12], and two additional chemical parameters were identified using experimental data published by Dillon and Murphy [11]. Four material parameters for the active mechanical response and five material parameters for the passive mechanical response were then determined by fitting mechanical experimental data. In the constitutive model proposed by Murtada et al. [17] two chemical parameters were estimated by the authors and five chemical parameters were fixed based on the work by Rembold and Murphy [31] and Hai and Murphy [12]. In addition, five material parameters for the active mechanical response and three material parameters for the passive mechanical response were also determined using mechanical experimental data. Like the above-cited mechano-chemical models, the constitutive model we presented here fits the mechanical experimental data well but with fewer parameters.

In formulating the proposed constitutive model, we assumed that the active stress of the SMCs can be computed from the stress of their connected ACFs. This assumption was made since there is no information about the SMC deformation within the tissue during contraction. Under this assumption, the active response of the tissue can then be described without introducing a kinetics model for the interaction of the myosin heads and thin filaments. Instead, based on the sliding filament theory, we assumed that there are three forces that generate contraction: a motor force that initiates contraction, an elastic force for the cross-bridge deformation, and a viscous force for the filament sliding. The resulting evolution law expressed by Eq. (11) for an isometric contraction and Eq. (13) for an isotonic contraction defines the deformation of

Table 1
Model parameters.

Experimental data	α (s^{-1})	β	a	f_c (s^{-1})	κ	γ	K (Mpa)	μ/ψ (deg)
Uniaxial data [17]	0.023	0.328	0.777	0.641	1.103	1.048	0.188	
Uniaxial data [10]	0.134	0.700	0.710	0.720	5.949	2.051	1.400	0.025
Biaxial data [18]	0.020	0.138	0.190	0.652	4.235	0.398	2.614	37.00

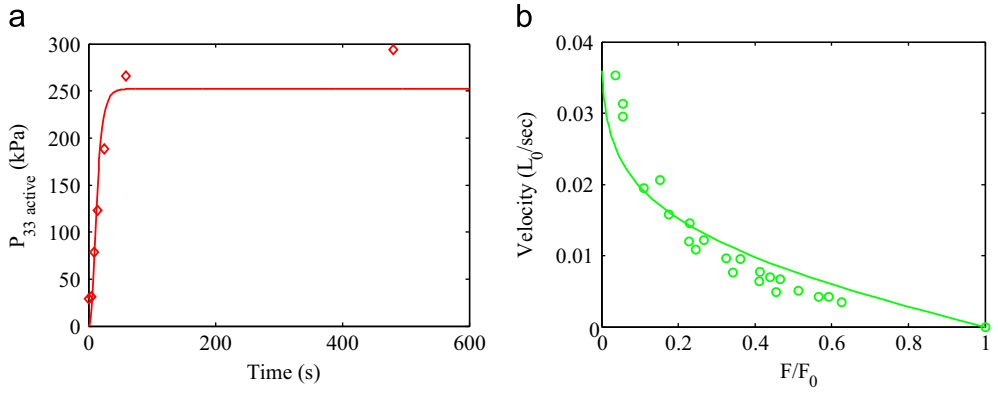

Fig. 3. Active and passive uniaxial data [10] and model fit ($R^2=0.922$). (a) Active stress–time experimental data (red symbols) at a stretch of 1.6 and model fit (continuous line); (b) velocity–force experimental data (green symbols) and model fit (continuous line). (For interpretation of the references to color in this figure caption, the reader is referred to the web version of this paper.)

Please cite this article as: T. Tan, R. De Vita, A structural constitutive model for smooth muscle contraction in biological tissues, International Journal of Non-Linear Mechanics (2015), http://dx.doi.org/10.1016/j.ijnonlinmec.2015.02.009

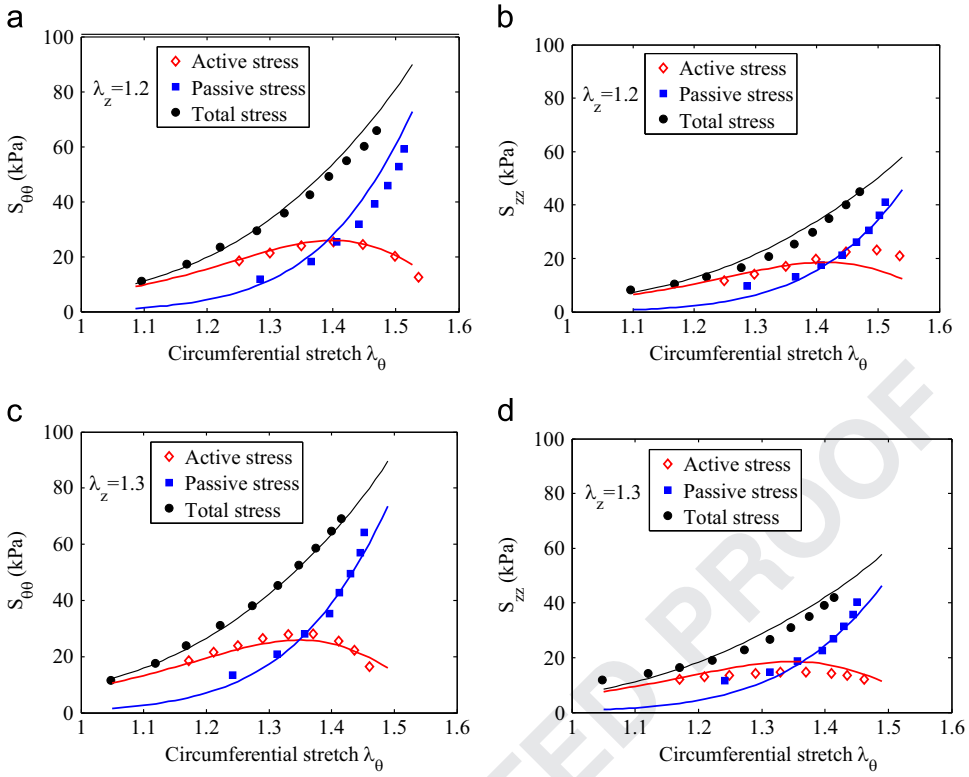

Fig. 4. Active and passive biaxial data [18] (R^2=0.965). (a) Active, passive, and total circumferential stress–stretch data at an axial stretch of 1.2 and model fits (continuous lines). (b) Active, passive, and total axial stress–circumferential stretch data at an axial stretch of 1.2 and model fits (continuous lines). (c) Active, passive, total circumferential stress–circumferential stretch data at an axial stretch of 1.3 and model fits (continuous lines). (d) Active, passive, and total axial stress–circumferential stretch data at an axial stretch of 1.3 and model fits (continuous lines).

ACFs with only four parameters. Three additional parameters were needed to describe the active and passive collagen fibers' mechanical behavior: two parameters for the recruitment of the fibers and one parameter for their elastic modulus. Overall, seven to eight parameters were needed to capture the results of uniaxial isotonic and isometric experiments on arteries.

The non-linearity in the active stress stemmed from the overlap mechanisms between the actin and myosin filaments for isometric contractions in the structural constitutive model by Murtada et al. [17]. These authors introduced a homogeneous parabolic function to describe this overlap mechanisms and, consequently, the active stress as a function of the tissue stretch had a parabolic profile. This led to underestimated values of the active stress when the tissue was stretched above the optimal stretch. In our study, the non-linearity in the active stress was assumed to be determined by the recruitment model that defined the stress of the ACFs. Because this stress was assumed to be equal to the stress of the SMCs (Fig. 1(c)), we did not need a description of the SMC deformation and, thus, of the overlap mechanism to compute the active stress. The recruitment model with a Weibull probability distribution function yielded a better fit of the active stress–stretch data following the optimal stretch.

The parameters that were found by curve fitting the model to three sets of experimental data on arteries [17,10,18] are reported in Table 1. The value of the parameter α computed by using the data by Murtada et al. [17] was comparable to the value computed using the data by Chen et al. [18], but lower than the value computed using the data by Dillon et al. [10]. For a higher α-value, the maximum stress during an isometric test was reached within a shorter interval of time. This can be observed from the experimental data in Fig. 2(a) and Fig. 3(a). As β increased, the stretch of the ACFs in isometric contractions increased as one can see from Eq. (11) and, consequently, the active stress increased too. The high β-value obtained from the data by Dillon et al. [10] was due to the high value of the active stress obtained in their experiments. The elastic modulus of the collagen fibers, K, had a lower value for the data published by Murtada et al. [17]. This lower K-value can be explained by the lower active stress reported by Murtada et al. when compared to that reported by Dillon et al. However, the K-value from the data by Murtada et al. was lower than the K-value computed from the data by Chen et al. [18] despite the lower active stress reported by these authors. This may be explained by the re-orientation of the collagen fibers that may occur during loading and was neglected in the present model. The value of a, which denotes the ratio of the initial axial displacement of the SMC contractile units to the axial tissue displacement, obtained from biaxial experimental data [18] was lower than that obtained from uniaxial experimental data [17,10]. Thus, the initial axial displacement of the SMC contractile units given by Eq. (9) is much lower along the two preferred collagen fiber directions than along the circumferential direction of the arteries. The values of the motor force f obtained from the three sets of experimental data [17,10,18] were comparable. Finally, the collagen fiber orientation angle ψ was found to be similar to the 39° angle reported by Chen et al. [18].

This study has several limitations that are worth mentioning. Thus far we have only tested the proposed constitutive model with uniaxial and biaxial experimental data considering specific deformations. We selected published data on arteries to identify the model parameters since the active and passive mechanical data on these biological tissues are the most complete sets of published data. Three dimensional data that characterize the active and passive mechanics of arteries and other biological tissues are needed to further evaluate the proposed model. Moreover, in the reference configuration, the collagen fibers and their connected SMCs have been assumed to be all aligned along one direction

Please cite this article as: T. Tan, R. De Vita, A structural constitutive model for smooth muscle contraction in biological tissues, International Journal of Non-Linear Mechanics (2015), http://dx.doi.org/10.1016/j.ijnonlinmec.2015.02.009

when testing the model with uniaxial data or two directions when testing the model with biaxial data. In fact, the collagen fibers and SMCs are oriented along different directions within the arteries and the probability density function $R(\mathbf{m})$ in Eq. (2) should be computed through techniques such as small angle light scattering [32] and histology [18]. Finally, the orientation of the contractile units within the SMCs should also be taken into consideration in the model development. Such orientation is important since the active force is generated along these units and transmitted, through filament anchor points on the cell membrane, to surrounding collagen fibers and ground substance. Information about the micro-structural changes of the contractile units during mechanical loading is crucial for developing robust micro-structural constitutive models. These models will provide a better understanding of the mechanism of smooth muscle contraction and, ultimately, improve the treatment of medical disorders such as hypertension, asthma, and pelvic floor disorders caused, in part, by a mechanical dysfunction of the SMCs.

6. Conclusions

We proposed a new structural constitutive model that characterizes the active and passive mechanical responses of biological tissues containing SMCs. The active response was attributed to the collagen fibers connected to the SMCs and the passive response was attributed to the remaining collagen fibers. A new evolution law for the collagen fibers that are connected to the SMCs and are thus activated with them was derived based on the sliding filament theory. The active force was assumed to be determined by an initial motor force, cross-bridge deformation, and filament sliding. The constitutive model was validated using uniaxial isometric and isotonic and biaxial isometric experimental data on arteries [10,17,18]. This study advanced our understanding of the active mechanical behavior of biological tissues containing SMCs.

Acknowledgments

Funding was provided by NSF CAREER Grant no. 1150397.

References

[1] C.Y. Kao, M.E. Carsten, Cellular Aspects of Smooth Muscle Function, Cambridge University Press, 1997.
[2] F. Ali, P.D. Paré, C.Y. Seow, Models of contractile units and their assembly in smooth muscle, Can. J. Physiol. Pharmacol. 831 (2005) 825–831.
[3] Y.C. Fung, Biomechanics: Mechanical Properties of Living Tissues, Springer-Verlag, New York, 1993.
[4] J.T. Herlihy, R.A. Murphy, Length–tension relationship of smooth muscle of the hog carotid artery, Circ. Res. 33 (1973) 275–283.
[5] J.J. Feher, Quantitative Human Physiology: An Introduction, Academic Press, Waltham, MA, 2012.
[6] H.E. Huxley, Electron microscope studies of the organisation of the filaments in striated muscle, Biochim. Biophys. Acta 12 (1953) 387–394.
[7] H.E. Huxley, The mechanism of muscular contraction, Science 164 (1969) 1356–1366.
[8] A.F. Huxley, R.M. Simmons, Proposed mechanism of force generation in striated muscle, Nature 233 (1971) 533–538.
[9] A.F. Huxley, Muscle contraction, J. Physiol. 243 (1974) 1–43.
[10] P.F. Dillon, M.O. Aksoy, S.P. Driska, R.A. Murphy, Myosin phosphorylation and the cross-bridge cycle in arterial smooth muscle, Science 211 (1981) 495–497.
[11] P.F. Dillon, R.A. Murphy, High force development and crossbridge attachment in smooth muscle from swine carotid arteries, Circ. Res. 50 (1982) 799–804.
[12] C.M. Hai, R.A. Murphy, Cross-bridge phosphorylation and regulation of latch state in smooth muscle, Am. J. Physiol. Soc. 254 (1988) C99–C106.
[13] A. Rachev, K. Hayashi, Theoretical study of the effects of vascular smooth muscle contraction on strain and stress distributions in arteries, Ann. Biomed. Eng. 27 (1999) 459–468.
[14] M.A. Zulliger, A. Rachev, N. Stergiopulos, A constitutive formulation of arterial mechanics including vascular smooth muscle tone, Am. J. Physiol. Heart Circ. Physiol. 287 (2004) H1335–H1343.
[15] J. Stålhand, A. Klarbring, G.A. Holzapfel, Smooth muscle contraction: mechanochemical formulation for homogeneous finite strains, Prog. Biophys. Mol. Biol. 96 (2008) 465–481.
[16] S.C. Murtada, M. Kroon, G.A. Holzapfel, Modeling the dispersion effects of contractile fibers in smooth muscles, Mech. Phys. Solids 58 (2010) 2065–2082.
[17] S.C. Murtada, A. Arner, G.A. Holzapfel, Experiments and mechanochemical modeling of smooth muscle contraction: significance of filament overlap, J. Theor. Biol. 297 (2012) 176–186.
[18] H. Chen, T. Luo, X. Zhao, X. Lu, Y. Huo, G.S. Kassab, Microstructural constitutive model of active coronary media, Biomaterials 34 (2013) 7575–7583.
[19] A.V. Hill, The heat of shortening and the dynamic constants of muscle, Proc. R. Soc. B 126 (1938) 136–195.
[20] R. De Vita, W.S. Slaughter, A structural constitutive model for the strain rate-dependent behavior of anterior cruciate ligaments, Int. J. Solids Struct. 43 (2006) 1561–1570.
[21] C. Truesdell, W. Noll, The Non-Linear Field Theories of Mechanics, Springer-Verlag, 1965.
[22] A. Arner, Mechanical characteristics of chemically skinned guinea-pig taenia coli, Pflügers Arch. 395 (1982) 277–284.
[23] H.T. Syyong, A. Raqeeb, P.D. Paré, C.Y. Seow, Time course of isotonic shortening and the underlying contraction mechanism in airway smooth muscle, J. Appl. Physiol. 111 (2011) 642–656.
[24] Y.C. Fung, K. Fronek, P. Patitucci, Pseudoelasticity of arteries and of its mathematical expression, Am. Physiol. Soc. (1979).
[25] K.E. Kamm, W.T. Gerthoffer, R.A. Murphy, D.F. Bohr, Mechanical properties of carotid arteries from DOCA hypertensive swine, Hypertension 13 (1989) 102–109.
[26] H. Jiang, K. Rao, A.J. Halayko, W. Kepron, N.L. Stephens, Bronchial smooth muscle mechanics of a canine model of allergic airway hyperresponsiveness, J. Appl. Physiol. 72 (1992) 39–45.
[27] K. Takamizawa, K. Hayashi, T. Matsuda, Isometric biaxial tension of smooth muscle in isolated cylindrical segments of rabbit arteries, Am. J. Physiol. 263 (1992) H30–H34.
[28] H.P. Wagner, J.D. Humphrey, Differential passive and active biaxial mechanical behaviors of muscular and elastic arteries: basilar versus common carotid, J. Biomech. Eng. 133 (2011) 051009-1–051009-10.
[29] A. Agianniotis, A. Rachev, N. Stergiopulos, Active axial stress in mouse aorta, J. Biomech. 45 (2012) 1924–1927.
[30] M. Kroon, A constitutive model for smooth muscle including active tone and passive viscoelastic behaviour, Math. Med. Biol. 27 (2010) 129–155.
[31] C.M. Rembold, R.A. Murphy, Myoplasmic [Ca2+] determines myosin phosphorylation in agonist-stimulated swine arterial smooth muscle, Circ. Res. 63 (1988) 593–603.
[32] J. Nagatomi, K.K. Toosi, J.S. Grashow, M.B. Chancellor, M.S. Sacks, Quantification of bladder smooth muscle orientation in normal and spinal cord injured rats, Ann. Biomed. Eng. 33 (2005) 1078–1089.

Please cite this article as: T. Tan, R. De Vita, A structural constitutive model for smooth muscle contraction in biological tissues, International Journal of Non-Linear Mechanics (2015), http://dx.doi.org/10.1016/j.ijnonlinmec.2015.02.009